JOURNAL OF APPLIED PHYSICS **115**, 17E120 (2014)

Putative quantum criticality in the $(Cr_{90}Ir_{10})_{100-y}V_y$ alloy system

P. R. Fernando,[1] A. R. E. Prinsloo,[1,a)] C. J. Sheppard,[1] and L. Lodya[2]
[1]*Department of Physics, University of Johannesburg, PO Box 524, Auckland Park 2006, South Africa*
[2]*Sasol Technology, Research and Development, 1 Klasie Havenga Road, Sasolburg 1947, South Africa*

(Presented 6 November 2013; received 23 September 2013; accepted 28 October 2013; published online 31 January 2014)

Quantum criticality (QC) in spin-density-wave antiferromagnetic Cr and Cr alloy systems is a topic of current interest. In the present study, V was used as a tuning parameter to drive the Néel transition temperature (T_N) of the $(Cr_{90}Ir_{10})_{100-y}V_y$ alloy series with $0 \le y \le 14.3$ to zero and search for effects of QC in the process. The magnetic properties and possible QC behaviour (QCB) in this alloy system were investigated through electrical resistivity (ρ), specific heat (C_p), and susceptibility (χ) measurements as a function of temperature (T), indicating that T_N is suppressed to zero at a critical concentration $y_c \approx 9$. The Sommerfeld coefficient (γ) is considered a key indicator of QCB and a peak is observed in $\gamma(y)$ at y_c on decreasing y through this concentration, followed by a sharp decreasing trend. This behaviour is reminiscent of that observed for γ of the prototypical $Cr_{100-x}V_x$ QC system and allows for the classification of y_c in the $(Cr_{90}Ir_{10})_{100-y}V_y$ alloy system as a possible QC point. © *2014 AIP Publishing LLC*. [http://dx.doi.org/10.1063/1.4863162]

Cr alloys with group-8 nonmagnetic transition metals such as Ru, Os, Rh, Ir, and Pt show large anomalies of magnetic origin in its physical properties at the phase transition temperatures.[1] These diluents increase the electron to atom (e/a) ratio of Cr, changing the spin-density-wave (SDW) phase of pure Cr from an incommensurate (I) to a commensurate (C) SDW phase on increasing the diluent concentration. Thus, the magnetic phase diagrams of these alloys usually contain the paramagnetic (PM) phase, the transverse (T) ISDW, and longitudinal (L) ISDW phases, as well as the CSDW phase. A triple point exists on the magnetic phase diagrams of these alloys where the ISDW, CSDW, and PM phases coexist.[1] LISDW, TISDW, and PM phases are observed for impurity concentrations (x) below the triple point concentration (x_L) in dilute Cr alloys with group-8 impurities, while a TISDW-CSDW phase transition line is present for $x > x_L$. The spin-flip phase transition at temperature T_{SF}, defined as the transition temperature between LISDW and TISDW magnetic phases, and the ISDW-CSDW magnetic phase transition at temperature (T_{IC}) of certain Cr alloys with group-8 nonmagnetic transition metals, are first order transitions.[1,2]

The magnetic phase diagrams of both the Cr-Re and Cr-Ru systems include possible superconducting properties, as well as quantum critical behaviour (QCB) for $x \gg x_L$.[1,3,4] These properties are strongly aligned with current interests as are reflected in recent literature.[3–9] However, much of the previous work on the $Cr_{100-x}Ir_x$ system focussed on alloys with concentrations close to $x_L = 0.16$, while not much attention was given to higher diluent concentrations.[1,10,11] This might be due to the difficulty in producing single phase body centred cubic (bcc) samples that were previously reported.[12] The Cr-Ir magnetic phase diagram was not fully explored and was still unknown for concentrations above 4 at. % Ir,[10–12] until recently when Fernando *et al.*[13] confirmed behaviour similar to that observed for the Cr-Re and Cr-Ru alloy systems for $x \gg x_L$.

Following a similar approach to that of Jacobs *et al.*[3] and Reddy *et al.*,[4] V was used as a tuning parameter in the present study to drive the Néel transition temperature (T_N) of the $(Cr_{90}Ir_{10})_{100-y}V_y$ alloy series with $0 \le y \le 14.3$ to zero and search for effects of QC in the process.

Polycrystalline ternary $(Cr_{90}Ir_{10})_{100-y}V_y$ alloys with $0 \le y \le 14.3$ were prepared by arc melting in a purified argon atmosphere from Cr, Ir, and V of mass fractional purities 99.999%, 99.99%, and 99.9%, respectively. Powder X-ray diffraction (XRD) analyses confirmed the bcc crystal structure. The actual elemental composition and homogeneity were determined using electron microprobe analyses. Electrical resistivity (ρ) and specific heat (C_p) were measured in the range $2 \le T \le 380$ K, using a standard Quantum Design (QD) Physical Properties Measurement System (PPMS) incorporating appropriate measurement options. Resistivity measurements for the temperature range $300 \le T \le 1000$ K were performed in an inert gas environment using the standard dc-four probe method with Keithley instrumentation. For samples with transitions in a range 300 K $\le T \le$ 700 K, the PPMS with the vibrating sample magnetometer (VSM) oven option was used to measure the susceptibility (χ) on heating in an applied magnetic field of 20 kOe. The QD Magnetic Property Measurement System (MPMS) was used to measure the magnetization for samples with transitions in the temperature range 2 K $\le T \le$ 390 K. These samples were zero field cooled (ZFC) to 2 K and measurements were taken on heating in an applied magnetic field of 50 Oe.

Figure 1(a) shows $\rho(T)$ curves for representative samples from the $(Cr_{90}Ir_{10})_{100-y}V_y$ alloy series. T_N-values were taken at the temperature accompanying the minimum in the $\rho(T)$ curves associated with the magnetic anomaly.[1] No additional low temperature minima, associated with impurity resonant effects (IRS),[1] are observed in the $\rho(T)$ curves of these alloys. In the case of the $(Cr_{90}Ir_{10})_{91.3}V_{8.7}$ alloy, the

a)E-mail: alettap@uj.ac.za

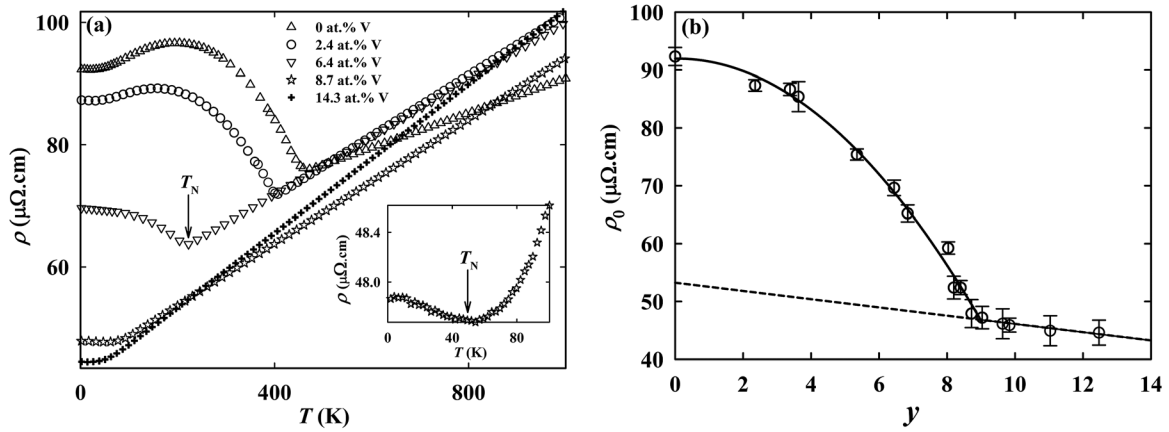

FIG. 1. (a) Electrical resistivity (ρ) as a function of temperature (T) for representative $(Cr_{90}Ir_{10})_{100-y}V_y$ alloys. The inset shows the low temperature anomaly observed for the $y = 8.7$ sample. (b) The y dependence of the residual resistivity, ρ_0, for the $(Cr_{90}Ir_{10})_{100-y}V_y$ alloys.

weak low temperature anomaly in the $\rho(T)$ curve (see inset of Fig. 1(a)) is therefore attributed to T_N rather than IRS. No minima were observed in the $\rho(T)$ curves of the alloys with $y > 9$ and it is assumed that these remain PM down to 2 K.

The residual resistivity, ρ_0, for each sample was obtained by extrapolation of the $\rho(T)$ curves from just above 2 K down to 0 K. Fig. 1(b) represents the ρ_0 behaviour as a function of V concentration, y. The dashed line represents a least square linear fit through the PM data points and corresponds to the $\rho_0(y)$ profile if the samples were all to remain PM down to 0 K. A similar decreasing trend in the ρ_0 data with increasing V content, as in Fig. 1(b), was also observed for $(Cr_{86}Ru_{14})_{100-s}V_s$.[4]

Figure 2 shows the $\chi(T)$ curves for representative $(Cr_{90}Ir_{10})_{100-y}V_y$ alloys. Anomalies, in the form of a downturn in $\chi(T)$ on cooling, are observed in the vicinity of T_N for the alloys with $y < 9$, similar to the behaviour normally observed for Cr alloys below T_N.[1,3] The dashed lines in Fig. 2 represent a back extrapolation from the PM phase at $T > T_N$ for each of the samples and the T_N values indicated by arrows were obtained from the point where the $\chi(T)$ curve deviates from the dashed line. $\chi(T)$ curves for alloys with $y > 9$ show no anomalous behaviour associated with a magnetic transition in the temperature range investigated. These samples were taken to be PM at all temperatures down to 2 K. It is interesting to note that the samples with $y = 3.4$, 3.6, and 5.4 showed two anomalies in their $\chi(T)$. The one anomaly occurs at a temperature that corresponds with the T_N obtained from the $\rho(T)$ measurements for these samples, while second anomaly, observed at a lower temperature, could possibly be attributed to a CSDW-ISDW transition that occurs on doping the $Cr_{90}Ir_{10}$ with V.

The values of the susceptibility at 293 K for these alloys are comparable with that obtained for the Cr + 10.7 at. % Re sample.[14] No clear trend is observed in the values of the susceptibility on increasing the diluent content, similar to that observed for Cr-Re[14] and Cr-V.[15] However, the T_N values obtained from the $\chi(T)$ curves in the present study show a pertinent decreasing trend on increasing the V content.

The behaviour of T_N and $(\Delta\rho_0/\rho_0)$ as a function of V concentration, y, is shown in Fig. 3. The T_N-values shown were obtained from $\rho(T)$ and $\chi(T)$ curves and indicate a critical concentration, y_c, for which T_N continuously tends to zero. The value of y_c was obtained from a fit to the experimental data (solid line in figure), using a power law of the form $T_N = a(y_c - y)^b$, where a and b are fitting parameters with: $a = (146 \pm 8)$ K, $b = 0.54 \pm 0.03$, and $y_c = 9.030 \pm (5 \times 10^{-6})$. The magnetic contribution to the residual resistivity of the AFM alloys, $\Delta\rho_0 = \rho_0 - \rho_{PM}$, where ρ_{PM} is the PM component of ρ_0, was obtained from the plot of $\rho_0(y)$, shown in

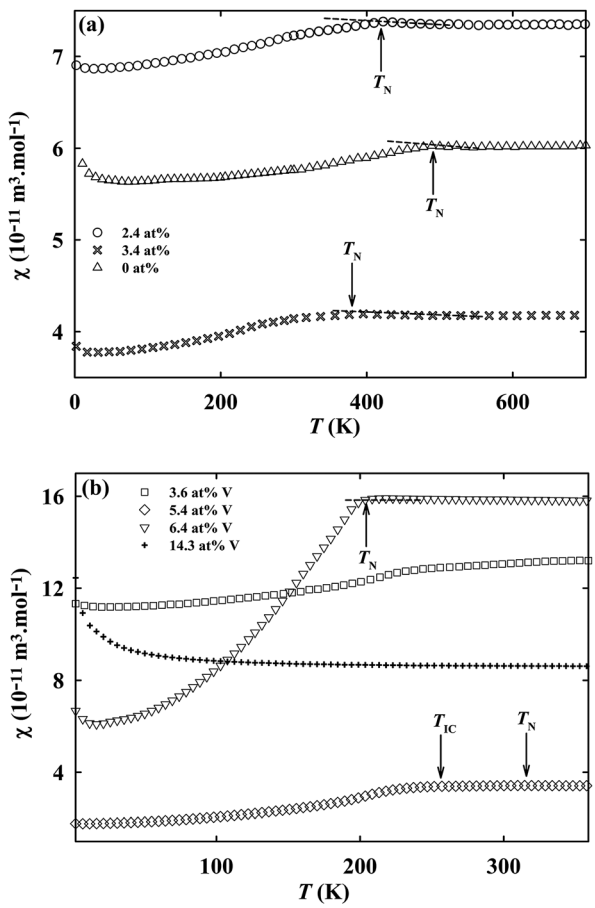

FIG. 2. The temperature dependence of the susceptibility, $\chi(T)$, of representative $(Cr_{90}Ir_{10})_{100-y}V_y$ alloys.

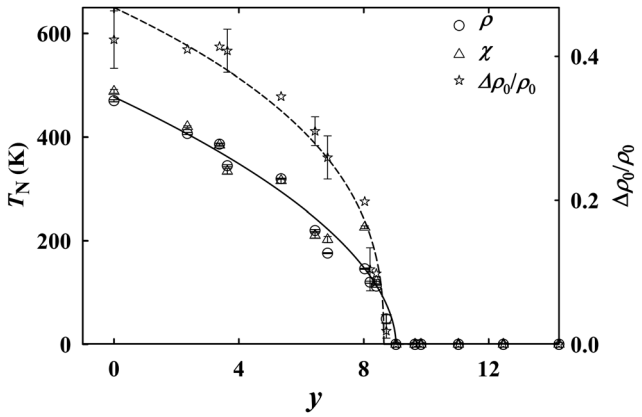

FIG. 3. T_N as a function of y for the $(Cr_{90}Ir_{10})_{100-y}V_y$ alloys obtained from $\rho(T)$ and $\chi(T)$ measurements. The solid line shows a power law fit through the $T_N(y)$ data. The star symbols give $\Delta\rho_0/\rho_0$ as a function of y, where $\Delta\rho_0$ is the magnetic contribution to the residual resistivity ρ_0. The dashed line shows a power law fit through the $\Delta\rho_0/\rho_0$ versus y data.

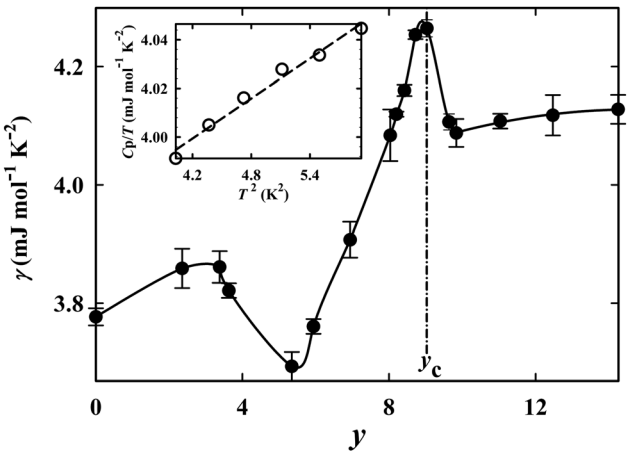

FIG. 4. The y dependency of the Sommerfeld electronic specific heat coefficient, γ. The solid line is a guide to the eye. The dotted dashed line indicates the position of y_c. The inset shows C_p/T versus T^2 for $y = 2.4$, with the dashed line depicting a least squares fit.

Fig. 1(b). On increasing y, $\Delta\rho_0/\rho_0$ in Fig. 3 decreases showing a sharp downturn towards zero close to y_c. A power law fit to the $\Delta\rho_0/\rho_0 - T$ data (dashed line in Fig. 3) indicates that this sharp downturn occurs at $y \approx 8.7$.

A key indicator of possible QC in Cr alloy systems is the behaviour of the Sommerfeld electronic specific heat coefficient (γ).[3,4,8,9] Fig. 4 depicts the y dependence of γ for the $(Cr_{90}Ir_{10})_{100-y}V_y$ alloy series. γ is obtained by fitting the low temperature C_p data to the equation $C_p = \gamma T + \beta T^3$ (example shown in the inset of Fig. 4 for $y = 2.4$). Here, the first term represents the electronic contribution to specific heat and the second term that of the lattice contribution. A deep minimum is observed in the $\gamma(y)$ curve of the present alloy series at $y \approx 5$, similar to that seen for the $(Cr_{84}Re_{16})_{100-z}V_z$ alloy system,[3] previously attributed to a possible CSDW–ISDW transition and supported by the present $\chi - T$ data. Following the deep minimum $\gamma(y)$ continuously increases for $y > 5$ reaching a maximum at $y \approx 9$, after which it decreases sharply for $y > y_c$, subsequently levelling off in the PM phase. This behaviour through y_c is reminiscent of that observed in the $Cr_{100-x}V_x$ system[9] for which $\gamma(x)$ increases sharply in the AFM ISDW phase up to the QC point (QCP), followed by a gradual decrease upon increasing x into the PM phase.

Electrical resistivity and susceptibility measurements on the $(Cr_{90}Ir_{10})_{100-y}V_y$ alloy system indicate that V doping of $Cr_{90}Ir_{10}$ suppresses T_N down to 2 K, and probably down to 0 K, near a critical concentration, $y_c \approx 9$, on the magnetic phase diagram. This is a necessary requirement for the occurrence of QC when tuning a magnetic system away from long-range order. Specific heat measurements were used to determine the Sommerfeld coefficient (γ) and $\gamma(y)$ shows a sharp increase up to y_c, resembling the behaviour observed for the archetypical $Cr_{100-x}V_x$ alloy system below the QCP. These results are taken as evidence for a putative QCP in the $(Cr_{90}Ir_{10})_{100-y}V_y$ alloy system at $y_c \approx 9$. Further studies, particularly extending the present studies to include other key indicators of QC such as Hall coefficient and Seebeck coefficient measurements, are already underway to confirm the suggestion of a QCP at $y_c \approx 9$ in the $(Cr_{90}Ir_{10})_{100-y}V_y$ alloy system. The present results should contribute to a broader understanding of QCB in Cr-alloys with group-8 nonmagnetic transition metals.

Financial support from the NRF (Grant 80928 and 80626) and UJ is acknowledged.

[1]E. Fawcett *et al.*, Rev. Mod. Phys. **66**, 25 (1994).
[2]E. Fawcett, Rev. Mod. Phys. **60**, 209 (1988).
[3]B. S. Jacobs *et al.*, J. Appl. Phys. **113**, 17E126 (2013).
[4]L. Reddy *et al.*, J. Appl. Phys. **103**, 07C903 (2008).
[5]A. Yeh *et al.*, Nature (London) **419**, 459 (2002).
[6]M. Lee *et al.*, Phys. Rev. Lett. **92**, 187201 (2004).
[7]R. Jaramillo *et al.*, Proc. Natl. Acad. Sci. U.S.A. **107**, 13631 (2010).
[8]C. J. Sheppard *et al.*, J. Appl. Phys. **109**(7), 07E104 (2011).
[9]J. Takeuchi *et al.*, J. Phys. Soc. Japan **49**, 508 (1980).
[10]J. Martynova *et al.*, J. Magn. Magn. Mater. **187**, 345 (1998).
[11]K. Fukamichi and H. Siato, J. Less-Common Met. **40**, 357 (1975).
[12]R. M. Waterstat and R. C. Manuszewski, J. Less-Common Met. **32**, 79 (1973).
[13]P. R. Fernando *et al.*, "Magnetic Phase Diagram of $Cr_{1-x}Ir_x$ alloys," in Proceedings of South African Institute of Physics Conference (2012).
[14]S. Arajs *et al.*, Phys. Status Solidi B **74**, K23 (1976).
[15]B. G. Child *et al.*, Philos. Mag. **5**(60), 1267 (1960).